crystals

MDPI

Article

Effect of (NbTi)C Particles on the Microstructure and Hardness of High Chromium and Nickel Indefinite Chilled Cast Iron

Hongwei Zhu [1], Shule Xia [2], Long Zhai [2], Jiyu Dong [1] and Furen Xiao [3,*]

[1] College of Physics & Electronic Science, Shanxi Datong University, Datong 037009, China; hwzhu@stumail.ysu.edu.cn (H.Z.); dongjiyu2814@163.com (J.D.)
[2] CITIC Dicastal Co., Ltd., Qinhuangdao 066004, China; xiashule@dicastal.com (S.X.); zhailong@dicastal.com (L.Z.)
[3] Key Laboratory of Metastable Materials Science & Technology, Hebei Key Laboratory for Optimizing Metal Product Technology and Performance, College of Materials Science & Engineering, Yanshan University, Qinhuangdao 066004, China
* Correspondence: frxiao@ysu.edu.cn; Tel./Fax: +86-335-8077110

Abstract: High chromium and nickel indefinite chilled cast iron (ICCI), as an excellent hot roll material, is the preferred roll variety due to its good combination of surface roughness, hot crack resistance, and hot wear resistance. The microstructure and hardness of ICCI roll materials with different contents of (NbTi)C particles is studied here, and the microstructure evolution process is analyzed by X-ray diffraction. The influence of (NbTi)C particles on the carbide morphology and distribution is investigated by metallographic microscopy and scanning electron microscopy, and the existence of (NbTi)C particles is observed. The experimental results show that (NbTi)C particles are present in granular, rod, and polygonal forms. Combined with a Thermo-Calc solidification phase diagram, it is found that the (NbTi)C particles undergo eutectic precipitation in the melt, forming short rod-shaped (NbTi)C carbides with a size of about 10 μm. Through the Rockwell hardness test, it is found that the hardness after adding 0.8 wt % (NbTi)C particles was 54.4 HRC, which was 21.1% higher than that without the addition.

Keywords: (NbTi)C particles; indefinite chilled cast iron; microstructure; hardness

check for updates

Citation: Zhu, H.; Xia, S.; Zhai, L.; Dong, J.; Xiao, F. Effect of (NbTi)C Particles on the Microstructure and Hardness of High Chromium and Nickel Indefinite Chilled Cast Iron. *Crystals* **2022**, *12*, 978. https://doi.org/10.3390/cryst12070978

Academic Editors: Marina Polyakova and Anton Meden

Received: 15 June 2022
Accepted: 12 July 2022
Published: 14 July 2022

Publisher's Note: MDPI stays neutral with regard to jurisdictional claims in published maps and institutional affiliations.

Copyright: © 2022 by the authors. Licensee MDPI, Basel, Switzerland. This article is an open access article distributed under the terms and conditions of the Creative Commons Attribution (CC BY) license (https://creativecommons.org/licenses/by/4.0/).

1. Introduction

High chromium and nickel indefinite chilled cast iron (ICCI) is an excellent material for hot rolling rolls, which has good wear resistance, anti-sticking, hot crack resistance and peeling resistance properties, and has become the first choice for the work rolls used for the rear stand of hot strip continuous rolling [1,2]. With the continuous expansion of rolling material specifications and varieties, and the increase of rolling speed, the rolling load gradually increases. It is imminent to develop high chromium and nickel ICCI with high wear resistance. A study has found that most of the cracks originate from the sharp corners of the carbide end [3]. Therefore, under the premise that without reducing the number of carbides to ensure wear resistance, one of the main ways to improve the performance of rolls is to reduce the occurrence of cracks and spalling by modifying the morphology of carbides [4,5].

The matrix microstructure of high chromium and nickel ICCI is composed of martensite and bainite, and there are many eutectic carbides, as well as a small amount of fine and well-dispersed graphite [6,7]. Increasing the amount of carbide can improve the hardness of the roll, and a small amount of graphite can ensure the self-lubrication of the roll [8]. By adding strong carbide forming elements, such as Nb, Ti, or V, to ordinary ICCI, fine granular carbides with high hardness can be obtained, so that the roll can maintain good accident resistance and improve the wear resistance at the same time [1,3,6,9,10]. The shape and size of austenite dendrites can also be improved, while this will lead to a decrease in the

hot cracking performance of ICCI. Tian et al. found that the lattice mismatch between rare earth oxides and primary austenite is very small, only 5.4% [11]. According to Bramfitt′s planar lattice disregistry theory, a small mismatch degree makes rare earth oxides enables the heterogeneous nucleation of primary austenite, which promotes a large degree of nucleation of primary austenite and achieves the effect of grain refinement [12]. Radulovic found that after the addition of a rare earth modifier, the number of primary austenite dendrites in ICCI increased, where the dendrite spacing decreased and the eutectic carbides were uniformly distributed in the matrix [13]. Li et al. further designed a RE-Nb composite modifier and found that rare earth materials can combine with oxygen, sulfur, and other harmful elements in molten iron to form fine oxides and sulfides which can purify the melt [14]. On the other hand, rare earth inclusions can be used as heterogeneous nucleation locations during the solidification of cast iron to improve the nucleation rate of primary grains and significantly refine the resulting cast microstructure, including reducing the columnar zone, expanding the equiaxed zone, and resulting in a microstructure with uniform and fine equiaxed grains. In addition, rare earth materials easily adsorb on the surface of eutectic carbides, which hinders the connection and growth of carbides, destroys the carbide network, and then forms rod-shaped and fishbone shaped carbides, passivating the sharp corners of carbides. The effect of stress concentration on the matrix can be reduced when subjected to external force to improve the service life of a roll [15–17]. However, Nb in the modifiers easily forms MC-type carbides with C in the melt, thus reducing segregation.

Although rare earth modifiers have achieved good modification effects, the prices of rare earth materials are expensive, which is not conducive to large-scale production. Therefore, the effect of a self-designed (NbTi)C modifier with different additions on the microstructure and hardness of high chromium and nickel ICCI was studied.

2. Materials and Methods

The base material used in this experiment is high chromium and nickel ICCI (GB/T 1504-2008, ICIV, C 2.90~3.60%, Si 0.60~1.50%, Mn 0.40~1.20%, P $\leq$ 0.10%, S $\leq$ 0.05%, Cr 1.00~2.00%, Ni 3.01~4.80%, Mo 0.20~1.00%, Shougang Jingtang Iron and Steel United Co., Ltd.) and its chemical composition was measured by a SPECTRO MAXx (LMX07) direct reading spectrometer, as shown in Table 1. The cast iron material was cut from a cylinder that was 20 mm in diameter into a small section with a length of 50 mm. The surface oxide skin and casting defects were polished with a grinding machine. The polished surface was cleaned with absolute ethanol. After drying with a blower, the base materials were placed in a vacuum drying oven at 200 °C for 2 h and were taken out before smelting. A vacuum medium frequency induction melting furnace with a rated power of 45 kW was adopted as the melting equipment. The crucible used a hot isostatic pressing magnesium oxide crucible with an inner diameter of 50 mm, an inner height of 100 mm, and a wall thickness of 10 mm. Before smelting, the crucible was wrapped with a glass fiber cloth with a temperature resistance of 2000 °C to prevent the melt flowing out and damaging the cooling system due to the crack of the crucible during the smelting process.

Table 1. Chemical composition of indefinite chill cast iron (wt %).

C	Si	Mn	P	S	Cr	Ni	Mo	V	Fe
3.40	0.70	0.92	0.041	0.026	1.76	4.50	0.40	0.023	Bal.

The preparation process of self-designed (NbTi)C particles has been introduced in detail in the literature [18–20]. Commercially available Nb powder, Ti powder (purity 99.5 wt % and particle size $\leq$ 40 μm), and graphite powder (purity 99.5 wt % and particle size $\leq$ 4 μm) were used as raw materials. The powder was ball milled for a total of 11 h using a planetary high-energy ball mill machine and then underwent annealing at 750 °C for 30 min. It should be noted that the ratio of Nb to Ti of the (NbTi)C particles in this paper was 0.8:0.2 and the particle diameter varies from 50 nm to 5 μm. Following this, cleaning

was performed for the furnace wall, sealing ring, material hopper, glass cover and other parts with alcohol, and the (NbTi)C particles were placed in the material hopper above the crucible. The particles were added into the crucible at 1580–1620 °C during smelting through the rocker control. The crucible was vacuumed after preparation and smelting began when the pressure reached 1.0×10^{-3} Pa. After smelting for about nine minutes, all materials had melted. The rocker was pulled to pour the (NbTi)C particles into the crucible and they were mixed for 2–4 min. During this process, the smelting temperature and pressure were kept stable. After smelting, the rocker was pulled to cast the material in the Al_2O_3 crucible (YAC0215, ∅ 88 × 107 mm, Qingdao Yaoxin Intelligent Technology Co., Ltd., Qingdao, China). Cast iron materials with the addition of (NbTi)C particles of 0, 0.15, 0.30 and 0.80 wt % were obtained.

The crystal structure and phase composition of ICCI were determined by an X-ray diffractometer (D/MAX-2500) with a scanning speed of 4°/min. The phase in the sample was calibrated by the MDI Jade 6.5 software package and PDF cards. The metallographic structure of the ICCI was observed and analyzed by an Axiover 200MAT microscope. The sizes and distributions of carbides in the ICCI were observed by a scanning electron microscope (SEM, S-4800-I), and the compositions of microscopic areas were analyzed by mapping scanning and energy dispersive spectroscopy (EDS). When preparing the sample, it was ground with paper ranging from 150 mesh to 2000 mesh SiC paper and was then mechanically polished with 0.5 μm diamond grinding paste, then using 1 g of picric acid, 5 mL of HNO_3, and 95 mL of absolute ethanol as corrosive agents. The Rockwell hardness was tested by HR-150A, and ten points were taken for each sample.

In order to analyze the solidification process of the ICCI and the influence of (NbTi)C particles on the phase transformation in detail, the Thermo-Calc 4.0 software package was used to calculate the phase diagram from 600 °C to 1600 °C based on the TCFE 7 database.

3. Results

3.1. Microstructure

The microstructure of ICCI is shown in Figure 1. It can be seen that the microstructure of ICCI without (NbTi)C particles is composed of light white carbides and dark black retained austenite inserted with needle-like martensite. The distribution of retained austenite shows dendritic characteristics, in which the primary dendrite is long and has obvious directionality, and the secondary dendrites are characterized by narrow and slender gaps between skeletons.

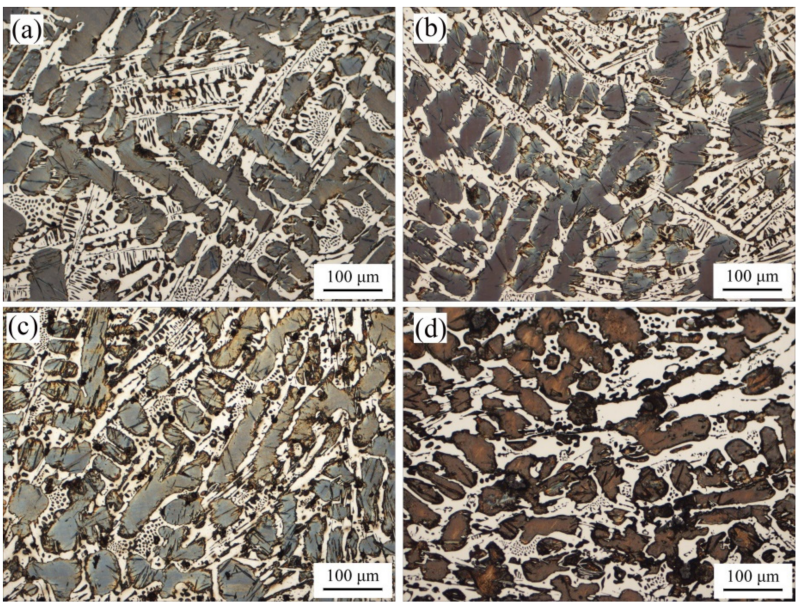


Figure 1. Metallographic images of the as-cast ICCI: (**a**) (NbTi)C-free; (**b**) 0.15 wt %; (**c**) 0.30 wt %; (**d**) 0.80 wt %.

In order to accurately determine the change trend of the retained austenite diameter, the Image-Pro Plus 6.0 software package was used for statistical analysis, and the results are shown in Figure 2. It can be seen from the analysis that the mean diameter decreased after the addition of (NbTi)C particles in varying degrees. The mean diameters for 0 wt %, 0.15 wt %, 0.30 wt %, and 0.80 wt % were 16.94 μm, 16.24 μm, 14.53 μm, and 15.49 μm, respectively. When the 0.15 wt % (NbTi)C particles were added, the size distribution of the retained austenite was heterogeneous. In addition, it can be seen in Figure 1 that with the increase of (NbTi)C particles, the distribution of retained austenite has no obvious directionality and the gaps between skeletons increase.

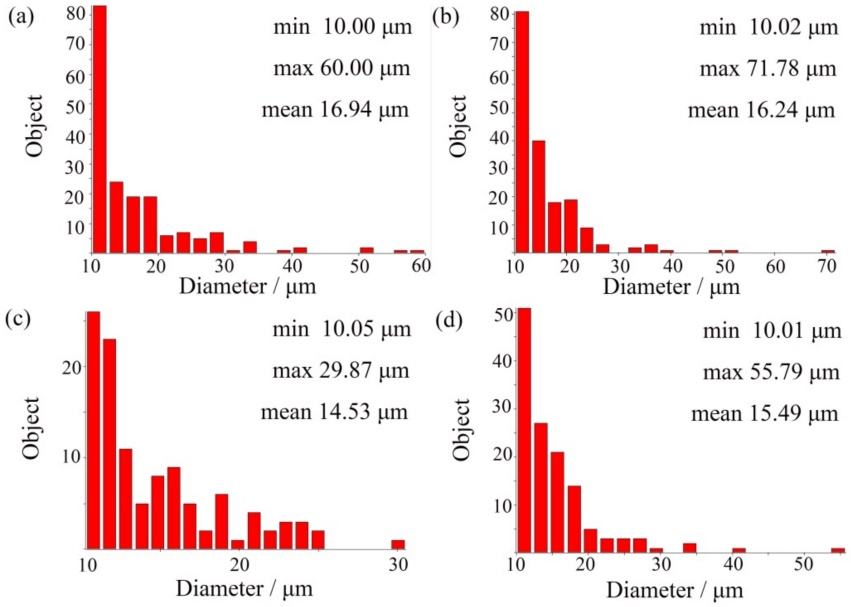


Figure 2. Frequency distribution histogram of retained austenite in ICCI: (**a**) (NbTi)C-free; (**b**) 0.15 wt %; (**c**) 0.30 wt %; (**d**) 0.80 wt %.

The X-ray diffraction results are shown in Figure 3. The microstructure of the ICCI without (NbTi)C particles shows a large amount of retained austenite and cementite, as well as a small amount of martensite. With the addition of (NbTi)C particles, the content of retained austenite decreased, while the content of martensite and cementite increased, which is consistent with the results in Figure 1.

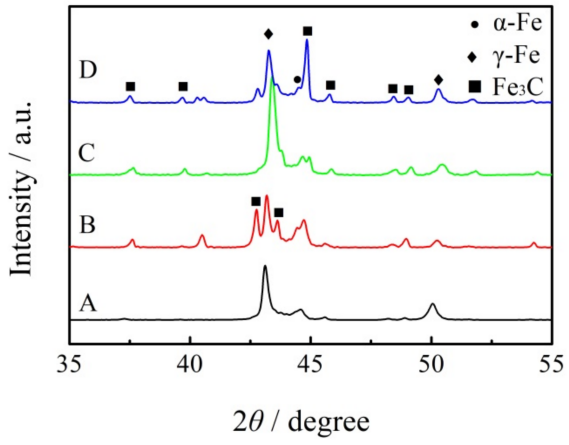


Figure 3. XRD patterns of as-cast ICCI. A, B, C and D is the spectral line of (NbTi)C particles added with 0, 0.15, 0.30 and 0.80 wt %, respectively.

In order to explore the distribution of (NbTi)C particles in ICCI in detail, the ICCI samples with a 0.30 wt % (NbTi)C addition were observed in terms of the backscattered electron (BSE) phase and were determined by EDS. Due to a small number of (NbTi)C particles observed, the samples with 0.15 wt % and 0.80 wt % (NbTi)C additions are not displayed here. The results are shown in Figure 4. The matrix features retained austenite, the gray black dendrite is cementite, and the bright white phase shows carbides with high atomic numbers. The morphology of particles distributed in grain and dendrites are dots that are 1–2 μm or rods with a length of about 10 μm.

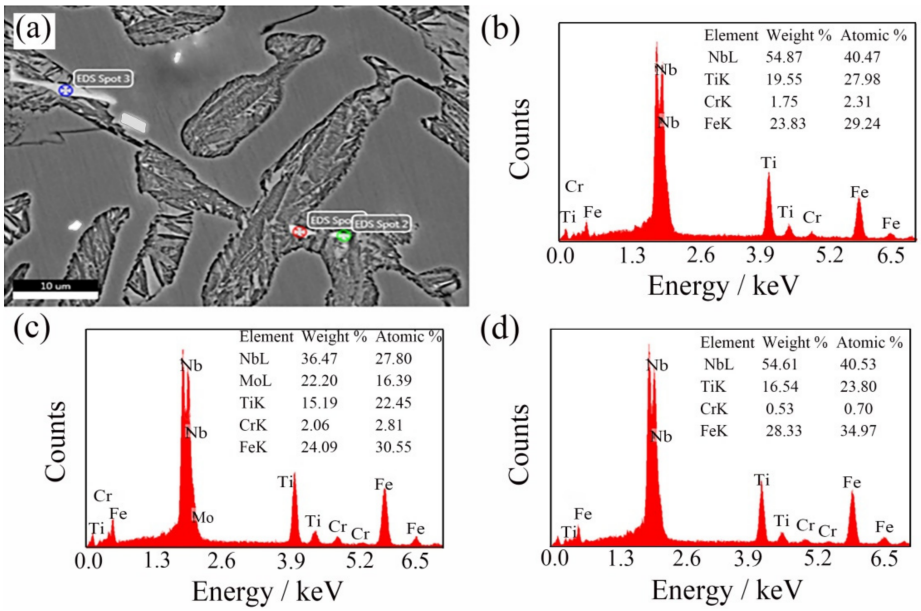


Figure 4. BSE observation after adding 0.30 wt % (NbTi)C particles (**a**) and the EDS of spot 1 (**b**), spot 2 (**c**), and spot 3 (**d**), respectively.

The results of the EDS mapping analysis are shown in Figure 5. It can be seen from the figure that some particles were distributed in the interior and boundaries of carbides, showing an angular structure mainly containing Nb and Ti elements. Cr is mainly distributed in carbides, while Ni is insoluble in carbides and is mainly distributed in retained austenite.

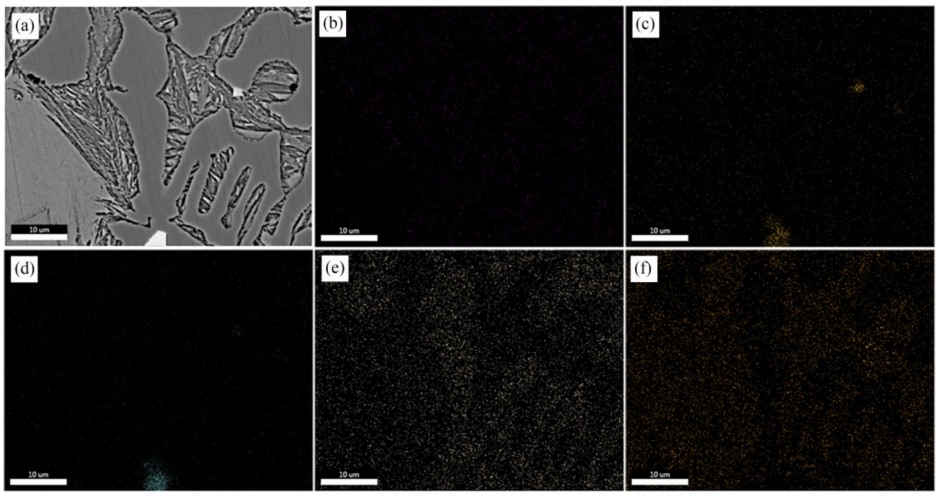


Figure 5. EDS mapping after adding a 0.30 wt % (NbTi)C sample: (**a**) SEM; (**b**) C; (**c**) Nb; (**d**) Ti; (**e**) Cr; (**f**) Ni.

3.2. Hardness

The hardness of the ICCI with different (NbTi)C particle additions was tested, and the results are shown in Figure 6. The hardness of the ICCI without (NbTi)C particles was 44.9 HRC. After adding the different (NbTi)C particles, the hardness results of the ICCI increased, reaching 51.1, 53.5, and 54.4 HRC for 0.15, 0.30, and 0.80 wt % additions, respectively, and the increase rates were 13.8%, 19.1%, and 21.1%, respectively. It is worth noting that the error of the hardness value is small, and the rising trend of the hardness value decreased with an increasing addition amount.

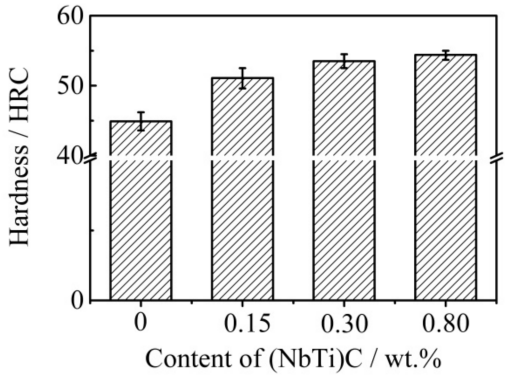


Figure 6. Hardness of the ICCI with different (NbTi)C particle contents.

4. Discussion

It can be seen from the microstructure that the sizes of the austenite and carbides decreased after adding (NbTi)C particles (Figure 1), and the main reason for this structural transformation may be because the (NbTi)C particles can be used as the nucleation core of austenite, which increases the nucleation probability of austenite. Previous studies have confirmed that the addition of (NbTi)C particles can host the nucleation position of austenite in carbon steel [18–20], and that the (NbTi)C particles can hinder the growth of primary austenite grains. In addition, research has shown that the added particles also have a certain refining effect on carbides in cast iron [21,22]. According to the semi-quantitative determination of EDS (Figure 4), the main elements of bright white particles are Nb and Ti. It can be preliminarily concluded that the constituent elements come from the added (NbTi)C particles. However, the morphologies and sizes of particles are different from the spherical (NbTi)C particles prepared, and the particles contain Mo and Cr.

In combination with the observation in Figures 4 and 5, the added (NbTi)C particles mainly exist in three forms here, except for a small amount in a solid solution: first, a granular form among dendrites (spot 1 and 2 in Figure 4a). The ratio of Nb to Ti in these particles is close to that in the added (NbTi)C, while the size is large except for mixing Cr and Mo elements; second, the sizes and morphologies of the rod-shaped particles (spot 3 in Figure 4a) between dendrites are different from those of the added (NbTi)C; finally, the third form is where the particles exist in polygonal forms with sharp edges and corners (Figure 5a). In order to explore the mechanism of (NbTi)C particle addition on the solidification process of the ICCI and the formation process of various forms (NbTi)C, the solidification process of ICCI was simulated by the Thermo-Calc software package (databases: TCFE7). The equilibrium phase diagram, phase fraction diagram, and mole fraction of solid phase diagram are shown in Figure 7. The equilibrium phase diagram and phase fraction diagram were calculated by the POLY module without considering the impurity of elements such as S and P. The mole fraction of the solid phase diagram was calculated using the SCHEIL module as per the Scheil–Gulliver model.

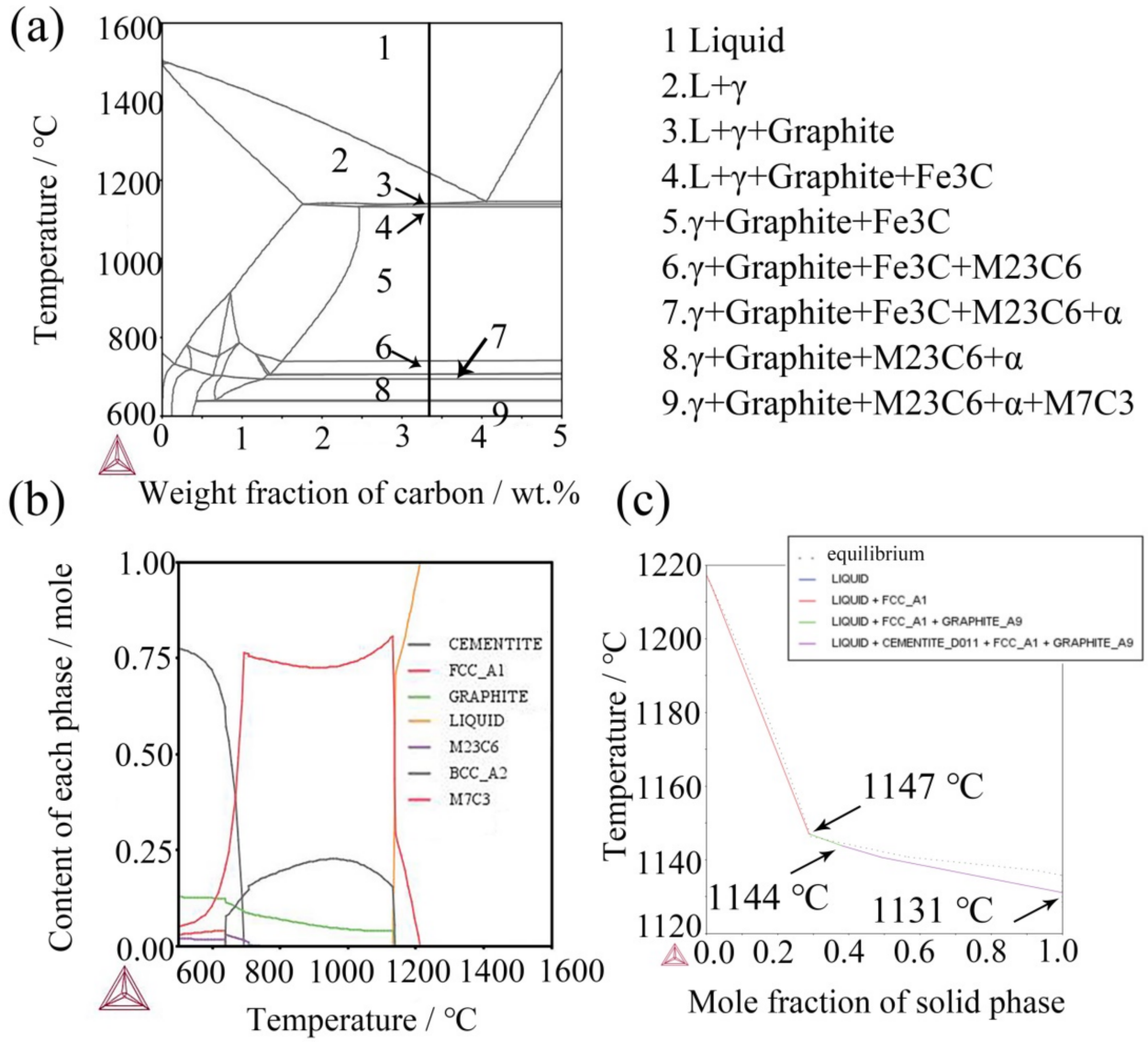


Figure 7. (**a**) Equilibrium phase diagram of ICCI: L-liquid, γ-austenite; (**b**) content of each phase fraction of ICCI; (**c**) non-equilibrium mole fraction of solid phase.

It can be seen from the phase diagram that during the solidification of the ICCI, the primary austenite precipitates from the liquid phase through homogeneous transformation at 1216 °C. At this time, the added (NbTi)C particles are used as nucleation cores, which increases the nucleation point of austenite and refines the austenite grains. This is consistent with the observation in Figure 1. According to particle repulsion theory, the (NbTi)C particles that do not become a nucleation core are repulsed by the austenite solidification front and are dispersed among the austenite dendrites. These kinds of (NbTi)C particles are segregated and grow with Mo and Cr elements at austenitic grain boundaries due to being pushed by the solidification front, which also hinders the grain growth of austenite (spots 1 and 2 in Figure 4a). With the progress of the solidification process, primary austenite is continuously precipitated and the solubility of C element in austenite (1.75%) is less than that in liquid phase (3.7%), which makes the content of C in the liquid phase gradually increase. When it reaches 4.3%, the eutectic transformation from liquid phase to austenite and cementite occurs, and the eutectic (NbTi)C particles are re-precipitated due to the dissolution of added (NbTi)C particles in the smelt, i.e., L→γ + (NbTi)C + Fe_3C.

Studies have shown that Ni can improve the stability of austenite, and when the content of Ni is higher than 4.5 wt %, it can prevent austenite decomposing into perlite and transforming into bainite or martensite [23,24]. The effect is more significant after adding Ni and Mo at the same time. Therefore, the microstructure of ICCI contains retained austenite and martensite.

The Cr content of ICCI in this paper was 1.76%, which mainly exists as M_3C carbides during solidification (Figure 5e). Studies have shown that when the Cr content is less than 7 wt %, it mainly exists in M_3C carbides, reducing the strength and deflection. When the Cr content increases, the carbides will change from $(Fe, Cr)_3C$ to $(Fe, Cr)_7C_3$ [25]. Therefore, the microstructure of the ICCI features M_3C-type carbides, and there is Cr segregation in the eutectic (NbTi)C particles with a rod-like dendrite gap in the restrained austenite (Figure 4a spot 3). In addition, in the residual liquid phase, (NbTi)C particles also become heterogeneous nucleation cores for cementite (Figure 5a), making the carbides finer and more uniform and reducing the number of network carbides.

In terms of hardness, the change of hardness of ICCI is caused by the microstructure. The Ni element in the ICCI enters into austenite, which improves the stability of the austenite and remains when transitioning to a normal atmospheric temperature, and part of the austenite transforms into martensite. Due to the refinement of austenite by (NbTi)C particles, the phase interface is increased. The refinement of carbides can reduce network carbides and the cleavage effect on the matrix and can improve the resulting hardness. With the increase of (NbTi)C particles, the refining effect is weakened, resulting in a slow increasing trend of hardness.

5. Conclusions

1. The addition of different contents of (NbTi)C particles can improve the microstructure of ICCI, including increasing the content of M_3C-type carbides and resulting in finer and more uniform dendrites, in which (NbTi)C particles exist as granules, rods of about 10 μm in length, and polygons.
2. The Thermo-Calc simulation has shown that during solidification, the γ phase, graphite, and Fe_3C precipitate in liquid phase in turn, and the liquid phase transformed into a solid phase at 1131 °C. The eutectic (NbTi)C particles may be formed in the transformation of $L \rightarrow \gamma$ + (NbTi)C + Fe_3C.
3. The hardness of ICCI increased with an increasing addition (NbTi)C particles. When the addition amount was 0.80 wt %, the hardness reached 54.4 HRC, which is 21.1% higher than that without addition, mainly due to the increase and refinement of carbides.

Author Contributions: Conceptualization, F.X. and H.Z.; methodology, F.X. and H.Z.; software, F.X. and H.Z.; validation, H.Z., S.X. and L.Z.; formal analysis, J.D.; investigation, H.Z., S.X. and L.Z.; resources, F.X. and S.X.; data curation, H.Z. and J.D.; writing—original draft preparation, H.Z.; writing—review and editing, H.Z. and F.X.; visualization, H.Z.; supervision, F.X.; project administration, F.X. and H.Z.; funding acquisition, F.X. and H.Z. All authors have read and agreed to the published version of the manuscript.

Funding: This research was funded by National Natural Science Foundation of China (Grant NO. 51971198), Hebei Province Innovation Ability Promotion Project (Grant NO. 22567609H), Science and Technology Innovation Project of Shanxi Colleges and Universities (Grant NO. 2021L385), Scientific Research Project of Shanxi Datong University (Grant NO. 2021YGZX34 and XJG2020231).

Institutional Review Board Statement: Not applicable.

Informed Consent Statement: Not applicable.

Data Availability Statement: Not applicable.

Conflicts of Interest: The authors declare no conflict of interest.

References

1. Kim, S.H.; Baek, E.R.; Jang, B.K. The effect of vanadium addition on the fracture and wear resistance of indefinite chilled cast iron. *Mater. Today Commun.* **2020**, *26*, 101819. [CrossRef]
2. Moonesan, M.; Raouf, A.H.; Madah, F.; Zadeh, A.H. Effect of alloying elements on thermal shock resistance of gray cast iron. *J. Alloys Compd.* **2012**, *520*, 226–231. [CrossRef]
3. Huang, G.Z.; Li, Z.H. Effect of vanadium and niobium on the microstructure of carbide reinforced indefinite chilled cast rolls. *Adv. Mater. Res.* **2011**, *311–313*, 864–870. [CrossRef]
4. Tercelj, M.; Fajfar, P.; Godec, M.; Kugler, G. Characteristics of the thermal fatigue resistance for 3.1C, 0.8Si, 0.9Mn, 1.7Cr, 4.5Ni and 0.3Mo ICDP cast iron roll at 600 °C. *Mater. Technol.* **2017**, *51*, 515–521. [CrossRef]
5. Ahiale, G.K.; Choi, W.D.; Suh, Y.; Lee, Y.K.; Oh, Y.J. Effect of MC-type carbide forming and graphitizing elements on thermal fatigue behavior of indefinite chilled cast iron rolls. *Metall. Mater. Trans. A* **2015**, *46*, 4819–4827. [CrossRef]
6. Huang, G.Z.; Shi, D.S.; Zhang, L.Y.; Li, Q. Effect of Nb and V contents on microstructure of carbide reinforced indefinite chilled rolls. *Heat Treat. Metals* **2014**, *39*, 58–62.
7. Bombac, D.; Kugler, G.; Markoli, B.; Tercelj, M. Hot work roller surface layer degradation progress during thermal fatigue in the temperature range 500–700 °C. *Int. J. Fatigue* **2017**, *104*, 355–365. [CrossRef]
8. Ha, D.J.; Sung, H.K.; Park, J.W.; Lee, S. Effect of alloying elements on microstructure, hardness, wear resistance, and surface roughness of centrifugally cast high-speed steel rolls. *Metall. Mater. Trans. A* **2009**, *40*, 2568. [CrossRef]
9. Bedolla-Jacuinde, A.; Correa, R.; Quezada, J.G.; Maldonado, C. Effect of titanium on the as-cast microstructure of a 16% chromium white iron. *Mater. Sci. Eng. A* **2005**, *398*, 297–308. [CrossRef]
10. Huang, Z.F.; Xing, J.D.; Zhi, X.H.; Gao, Y.M. Effect of Ti addition on morphology and size of primary M_7C_3 type carbide in hypereutectic high chromium cast iron. *Mater. Sci. Technol.* **2011**, *27*, 426–430. [CrossRef]
11. Tian, Y.J.; Wu, H.Q.; Guo, J.H.; Li, F.R. Effect of RE inclusions on heterogeneous nucleation of primary austenite in Fe-C alloys. *J. Chin. Rare Earth Soc.* **1988**, *6*, 45–48.
12. Bramfitt, B.L. Planar lattice disregistry theory and its application on heterogistry nuclei of metal. *Metall. Trans.* **1970**, *1*, 1987–1995. [CrossRef]
13. Radulovic, M.; Fiset, M.; Peev, K. Effect of rare earth elements on microstructure and properties of high chromium white iron. *Mater. Sci. Technol.* **1994**, *10*, 1057–1062. [CrossRef]
14. Li, C.H.; Song, Y.P.; Wei, X.; Lu, C.; Liu, B.C.; Han, Y.T. Effect of heat treatment on microstructures and properties of RE-Nb modification chilled cast iron. *Spec. Cast. Nonferrous Alloy.* **2014**, *34*, 623–625.
15. Guo, E.; Wang, L.; Huang, Y. Effect of RE, V, Ti, and B composite modification on the microstructure and properties of high chromium cast iron containing 3% molybdenum. *Rare Met.* **2009**, *28*, 6. [CrossRef]
16. Yang, F.; Xia, P.; Kou, X.; Wang, Y.; Zhang, W. Effect of RE-Al compound modifier on microstructure and properties of Ni-Cr-Mo chilled cast iron used for casting roll. *Foundry Technol.* **2015**, *36*, 972–976.
17. Gou, J.; Wang, Y.; Wang, C.; Chu, R.; Liu, S. Effect of rare earth oxide nano-additives on micro-mechanical properties and erosion behavior of Fe-Cr-C-B hardfacing alloys. *J. Alloys Compd.* **2017**, *691*, 800–810. [CrossRef]
18. Zhu, H.W.; Ke, W.J.; Zhao, Z.P.; Qin, S.; Xiao, F.R.; Liao, B. Refinement effectiveness of self-prepared (NbTi)C nanoparticles on as-cast 1045 steel. *Mater. Des.* **2018**, *139*, 531–540. [CrossRef]
19. Zhu, H.W.; Xu, K.; Qin, S.; Xiao, F.R.; Liao, B. Effect of heat treatment on microstructure and properties of 1045 steel modified with (NbTi)C nanoparticles. *Mater. Sci. Eng. A* **2018**, *728*, 175–182. [CrossRef]
20. Zhu, H.W.; Li, H.N.; Xiao, F.R.; Gao, Z.X. Study on the dissolution and precipitation behavior of self-designed (NbTi)C nanoparticles addition in 1045 steel. *Metals* **2021**, *11*, 184. [CrossRef]
21. Liu, S.; Zhou, Y.; Xing, X.; Wang, J.; Yang, Q. Refining effect of TiC on primary M_7C_3 in hypereutectic Fe-Cr-C harden-surface welding coating: Experimental research and first-principles calculation. *J. Alloys Compd.* **2017**, *691*, 239–249. [CrossRef]
22. Liu, S.; Zhang, J.; Wang, Z.; Shi, Z.; Zhou, Y.; Ren, X.; Yang, Q. Refinement and homogenization of M_7C_3 carbide in hypereutectic Fe-Cr-C coating by Y_2O_3 and TiC. *Mater. Charact.* **2017**, *132*, 41–45. [CrossRef]
23. Song, Y.; Cui, J.; Rong, L. Microstructure and mechanical properties of 06Cr13Ni4Mo steel treated by quenching–tempering-partitioning process. *J. Mater. Sci. Technol.* **2015**, *32*, 189–193. [CrossRef]
24. Sun, G.F.; Liu, C.S.; Tao, X.Q.; Chen, S.Y. Research on laser alloying of high-Ni-Cr infinite chilled cast iron roller. *J. Northeast. Univ.* **2008**, *29*, 845–848.
25. Zheng, B.; Xing, J.; Li, W.; Tu, X.; Jian, Y. Effect of chromium-induced $(Fe,Cr)_3C$ toughness improvement on the weo-body abrasive wear behaviors of white cast iron. *Wear* **2020**, *456–457*, 203363. [CrossRef]